photonics

Review

Advances on Solid-State Vortex Laser

Zhichao Zhang [1,2,3], Lan Hai [1,2,3], Shiyao Fu [1,2,3,*] and Chunqing Gao [1,2,3]

1 School of Optics and Photonics, Beijing Institute of Technology, Beijing 100081, China; 3120200603@bit.edu.cn (Z.Z.); 3120215336@bit.edu.cn (L.H.); gao@bit.edu.cn (C.G.)
2 Key Laboratory of Information Photonics Technology, Ministry of Industry and Information Technology of the People's Republic of China, Beijing 100081, China
3 Key Laboratory of Photoelectronic Imaging Technology and System, Ministry of Education of the People's Republic of China, Beijing 100081, China
* Correspondence: fushiyao@bit.edu.cn

Abstract: Vortex beams (VBs) are structured beams with helical wavefronts carrying orbital angular momentum (OAM) and they have been widely used in lots of domains, such as optical data-transmission, optical tweezer, quantum entanglement, and super-resolution imaging. The ability to generate vortex beams with favorable performance is of great significance for these advanced applications. Compared with extra-cavity schemes, such as spatial light modulation, mode conversion, and others which transform other modes into vortex modes, solid-state vortex lasers can output vortex beams directly and show advantages including a compact structure, high robustness, easy to integrate, and low cost. In this review, we summarize intra-cavity generation approaches to vortex beams in solid-state lasers. Our work on 1.6μm eye-safe vector vortex lasers is also introduced.

Keywords: orbital angular momentum; vortex beam; solid-state laser; intra-cavity generation

Citation: Zhang, Z.; Hai, L.; Fu, S.; Gao, C. Advances on Solid-State Vortex Laser. *Photonics* **2022**, *9*, 215. https://doi.org/10.3390/photonics9040215

Received: 28 February 2022
Accepted: 22 March 2022
Published: 24 March 2022

1. Introduction

Laser field manipulation is currently one of the hot topics in the photonics community [1]. A variety of beams, e.g., frequency comb, beam lattices, and ultrafast laser, can be obtained through tailoring multiple degrees of freedom, such as frequency [2], complex amplitude [3–5], and time [6,7], respectively. Vortex beams obtained by tailoring their total angular momentum (TAM) have caught the increasing attention of researchers around the world [8–13]. Over the past 30 years, research into vortex beams has gone through different stages, from scalar to vector, from phase singularity to polarization singularity. Early in 1992, Allen et al. proved that a beam whose complex amplitude comprises the helical phase term $\exp(il\varphi)$ carries OAM $l\hbar$ per photon [14], where l denotes the topological charge, φ denotes the azimuthal angle, and $\hbar$ is Planck's constant divided by 2π. Such a beam has a phase singularity in the center leading to a doughnut intensity pattern, and is thus called a phase vortex or scalar vortex beam. Since then, the attractive properties of vortex beams have been continually excavated [15–20] to inspire many applications, such as optical communications [21–28], rotation detection [29–36], optical tweezers [37–41], and so on. With the development of laser field manipulation, a new structured beam, vector vortex beams (VVBs), came to peoples' attention [42,43]. Compared with the scalar vortex beams, they have similar but distinguishing modes with non-separable states in which spin angular momentum (SAM) and orbital angular momentum (OAM) are coupled. Such a property results in anisotropic polarization, where additional polarization singularities are present. Consequently, VVBs have shown great potential for quantum technologies [44–47] and electron and plasma beams [48,49] in the last decade. Moreover, they have been applied in other promising applications, such as laser processing [50,51], high-resolution imaging [52], surface plasmon excitation [53], etc. Note that in this paper, scalar and vector vortex beams are collectively called vortex beams.

The ability to generate above vortex beams with favorable performance is of great significance for their advanced applications [54–57]. Lots of schemes have been demonstrated where the technical route can be divided into passive and active methods, corresponding to extra-cavity and intra-cavity generation. The research of passive methods began in the 1990s, using spatial devices outside the laser resonator to modulate the phase of the Gaussian beam, so as to obtain the scalar and vectorial vortex beams. The commonly used approaches are involved with classical optical elements, including mode convertor [58,59], spiral phase plate (SPP) [60–64], computer-generated holograms [65–67], and more recently novel metasurfaces [16,68–71], digital micromirror devices (DMD) [72–74], and Q-plate (QP) [75], etc. Actually, in the past decades, our group has done a lot regarding passive vortex beam generation, e.g., demonstrating the Twyman Green interferometer [76], Sagnac-like interferometer [77], cascaded spatial light modulation [78], and programable vortex source [79,80]. Generally speaking, the above schemes are relatively mature. More recently, researchers have paid increasing attention to active vortex generation schemes such as the vortex laser, including solid-state laser, fiber laser [81], on-chip vortex laser [82], and vertical-cavity surface-emitting lasers (VCSELs) [83,84]. Among them, solid-state vortex lasers show advantages, including compact structure, high efficiency, and low cost. Besides, the high-order transverse mode of the controllable time characteristic can also be easily obtained. Moreover, since beams located at 1.6μm operate in the eye-safe spectral range and are attractive for atmospheric applications, such as wind field velocity mapping [85] and atmospheric pollution monitoring [86], lots of attention has also been paid recently to developing single frequency Er:YAG vortex lasers.

This paper mainly reviews recent advances in solid-state vortex laser. In Section 1, a brief introduction about vortex beams and their commonly generation schemes are presented. Considering the rapid development of solid-state laser, the intra-cavity methods of vortex beam generation, including annular pumping, off-axis pumping, and other kinds, are reviewed in the following Section 2. In this section, we also introduce the generation of vector vortex laser in the eye safety band by inserting intra-cavity modulation devices, where our previous work on this issue is mainly presented. Finally, the conclusion and future prospects are presented in Section 3.

2. Vortex Lasers from Intra-Cavity Modulation

Intra-cavity vortex generation is used to suppress the Gaussian mode by controlling the relationship between gain and loss in the cavity, so as to generate the vortex laser. For example, methods based on gain control include annular pumping and off-axis pumping, and those based on loss manipulation include exploiting the thermal lens effect of the gain medium and inserting modulation devices in the cavity.

2.1. Annular Pumping

Annular pumped lasers for vortex beam generation were pioneered in 2001 [87]. Their principles are interpreted as spatial modulation devices can change the transverse distribution of a pump beam, so as to control the spatial distribution of gain in the crystal. By changing the gain distribution of different intrinsic modes in the cavity and increasing the gain of a specific intrinsic mode, the control of the specific intrinsic mode generation of the resonator can be selectively controlled. Hitherto, in solid-state lasers, there have been some common methods to generate vortex beams by applying annular pumping, in which the annular pumping profiles are formed by a hollow mirror [88–91], optical fiber [87,92–98], diffractive optical device [99–101], cone lens [102], etc.

Using a hollow mirror to obtain an annular pump is an effective way. In 2016, Liu et al. reported an Er:LuYAG solid-state vortex laser in the case of continuous-wave (CW) laser operation [88,89]. The $LG_{0,\pm1}$ mode vortex beams were respectively realized through being pumped by an annular beam, which was reformatted by a specially fabricated optical mirror with high reflectivity and center-punched structure, as shown in Figure 1a. Then, combined with volume Bragg grating (VBG) and uncoated YAG crystal plate, 8.4 nm wavelength tunable width of five OAM states can also be achieved [90]. Later, in 2017, the same group demonstrated an Er:YAG ceramic solid-state laser pumped by above annular beam [91], which can control vortex helicity with a quarter-wave plate (QWP). As a result, up to 4.3 W of $LG_{0,+1}$ mode and 3.8 W of $LG_{0,\pm1}$ mode at 1645 nm were successfully obtained.

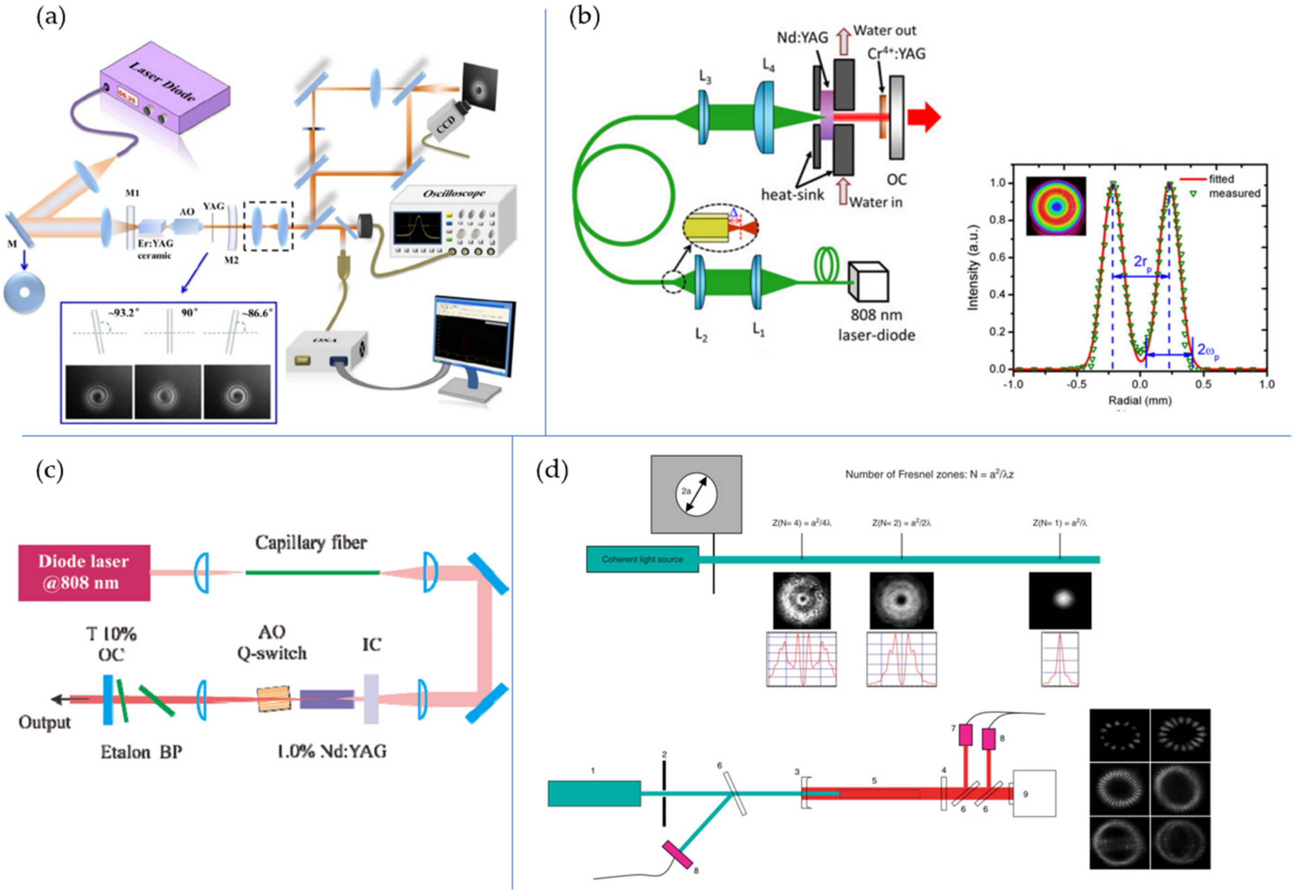

Figure 1. Annular-pumped vortex lasers. The annular pump beam is produced through (**a**) hollow mirror (Reprinted with permission from [88] © The Optical Society), (**b**) multi-mode fiber combined with defocusing characteristic (Reprinted with permission from [92] © 2015 Elsevier B.V), (**c**) capillary fiber (Reprinted with permission from [96] © The Optical Society), and; (**d**) diffractive optical device (Reprinted with permission from [99] © 2005 by Astro Ltd.).

Compared with a hollow mirror, optical fibers are more commonly exploited in annular pumping. In 2001, Chen et al. demonstrated that when a multi-mode fiber-coupled diode laser beam passes through a focusing lens, the profile at the focal plane is like a top-hat distribution [87]. However, away from the focal plane, it is like a doughnut-shaped distribution. With this property, pure $LG_{0,1}$ modes with the highest topological charge of 23 are generated in an end-pumped laser by defocusing a standard fiber-coupled diode to produce a doughnut-shaped pump profile. Considering the polarization characteristic, in 2015, Fang et al. demonstrated an annular-pumped Nd:YAG laser that emitted radially polarized $LG_{0,1}$ mode beam [92,93]. Figure 1b shows the schematic diagram of the experimental setup. By adjusting the distance between lens L2 and multi-mode optical fiber, the pump beam was reshaped into annular intensity distribution, then delivered into the laser cavity. In addition, by slightly tilting the laser's output coupler (OC), the vortex helicity can be controlled. Moreover, by tilting laser crystal, the polarization state can be switched from radial polarization to azimuthal polarization.

The schemes mentioned above mainly concern a multi-mode fiber combined with a defocusing characteristic. Another scheme involves applying capillary fiber to directly modulate a Gaussian beam into an annular beam. In 2012, Kim et al. employed a low-loss fiber beam-shaping element, i.e., an in-house-made capillary fiber with an air-hole in the center, to re-format the pump beam into a near-field annular intensity distribution beam, [94]. This re-formatted pump beam was spatially matched to the intensity distribution for the $LG_{0,1}$ mode in the Nd:YAG laser crystal. Hence, the high power $LG_{0,1}$ mode was generated directly from the laser resonator since it has the lowest threshold. In the following research, $LG_{0,1}$, $LG_{0,2}$, and $LG_{0,3}$ modes of 808 nm were obtained by the same group [95], respectively. Moreover, based on the solid-state laser technique, Q-switched lasers using the same pump have also been proposed, as shown in Figure 1c [96].

Diffractive optical devices are also employed to achieve annular pumping. In 2005, Bisson et al. demonstrated a 1.06 μm Nd:YAG laser pumped by a small hollow beam [99], which provided a high value of topological charge l of more than 200 for the $LG_{0,1}$ mode, as shown in Figure 1d. The hollow-shape intensity distribution in the near field was produced by diffracting the initial pump beam at a circular diaphragm. This scheme made it possible to change the distribution of pumping intensity and the inversion profile inside the active element by adjusting the distance z between the diaphragm and the active element. To optimize the structure, in 2016, Li et al. proposed and demonstrated an efficient vortex Nd:YVO_4 laser under the utilization of a circle Dammann grating (CDG) [100]. The CDG can diffract the incident beam into a single ring or multi-concentric ring with equal intensities at the far field. Therefore, with the pump beam from a LD incident in a first-order CDG, the obtained first-order diffraction ring profile could be used as the annular pumping field of a $LG_{0,1}$ mode solid-state laser. With the development of novel devices, in 2019, Schepers et al. presented a spatial gain shaping method that applies DMD as a shaping tool for the pump beam [101], enabling a high degree of freedom for the gain distributions that can be generated. More than 1000 high-purity Hermitian-Gaussian modes was realized.

Besides, Dong et al. designed a new type of annular focusing lens [103], through which the fundamental mode Gaussian beam can form a focused hollow pump beam directly. Using this annular pump, vortex beams with high optical conversion efficiency and high beam quality can be generated in solid-state lasers.

2.2. *Off-Axis Pumping*

Off-axis pumping can also generate vortex beams, whose advantages include low cost, easy realization, and high integration. The overlap rate of the pump and different mode distributions can be changed to generate the required high-order modes through controlling off-axis pumping. Then, a vortex beam carrying OAM is obtained through the mode astigmatism converter outside the cavity [104]. In 1996, Laabs et al. hit the pump beam through the optical fiber at different off-axis positions of the crystal [105]. When the pump overlap rate of a particular mode in the cavity reaches the highest, the gain is the highest but the loss is the lowest. So, specific modes can be selected. As a result, $HG_{0,0}$ to $HG_{0,87}$ modes are produced. In 2008, Chu et al. combined the off-axis pumping technique with a mode converter to convert high-order HG beams into LG beams with a maximum topological charge of 4, as shown in Figure 2 [106].

Since then, a series of solid-state lasers based on this method has been proposed. In 2018, Chen et al. used the off-axis pumping method by controlling the angle of the crystal to make the vortex beams have higher gain, so the vortex beams were selected to oscillate and output directly from the cavity [107]. An off-axis pumped laser was built and vortex beams with topological charge of 1 obtained by rotating the angle of the gain crystal were realized. In the same year, Wang et al. used the off-axis pumping method by adjusting the angle of the mirror to control the superposition of different Hermite–Gaussian beams in the cavity and generated vortex beams directly with double singularities [108]. In 2019, Lin et al. proposed a monolithic Nd: YAG nonplanar ring laser for spontaneous generation of vortex beams [109]. By the off-axis pumping scheme on the coated surface of the NPRO, LG mode lasing has been established. In 2021, Lin et al. built a set of off-axis pumped Tm:YLF solid-state laser, where 2 μm high-order vortex beams were generated for the first time [110].

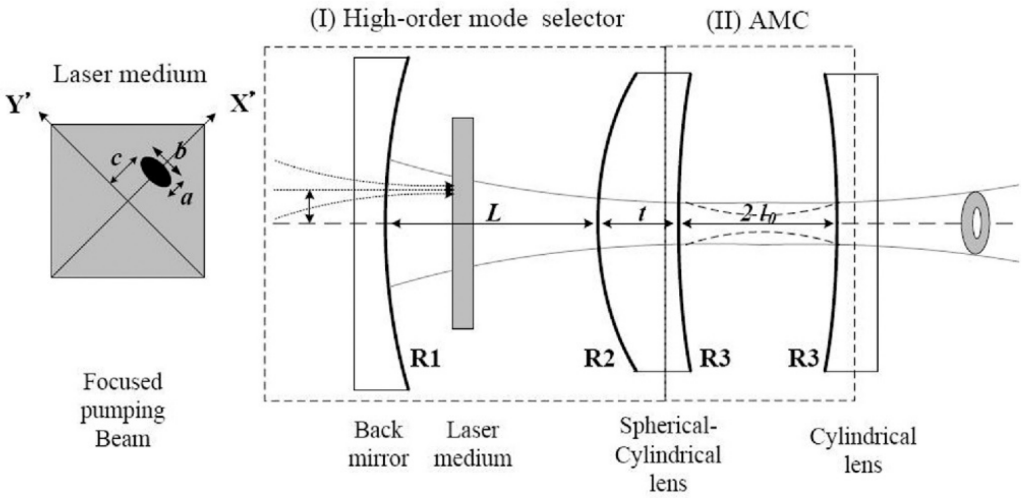

Figure 2. A $Nd:GdVO_4$ microchip laser with off-axis pumping and a mode converter [106]. Reprinted with permission from [106] © The Optical Society.

Furthermore, to obtain wave-versatile optical vortex beams, Liu et al. proposed a solid-state vortex laser utilizing a dual-off-axis pumped ultra-wide-band Yb:CALGO laser scheme [111], reaching a wavelength-tunable width of over 10 nm. This system was adapted to generate tunable dual-wavelength vortex beams.

2.3. Defect Mirror

The spot defect mirror scheme as a type of loss manipulation has outstanding advantage in intra-cavity generation of high order vortex beams with high quality and high stability. Since the high-order transverse mode beam expands spatially more than the low-order transverse mode, a spot defect mirror with proper size can suppress the Gaussian mode, or even the low-order transverse mode, so as to generate the required high-order transverse mode beam.

The key to this technique is a proper match between the damage spot diameter and the resonator mode size. In 2010, using defect-mirrors with appropriate damage spots to generate vortex beams was demonstrated in Nd:YAG lasers [112]. In 2013, Omatsu et al. demonstrated the direct generation of vortex beams from a CW, diode-end-pumped 1.06 μm $Nd:GdVO_4$ laser system [113]. The laser system consisted of a $Nd:GdVO_4$ crystal whose incident surface coated high reflectivity (HR) for 1064 nm and a concave OC with a laser-micro-machined circular damage spot of 40 μm diameter. Precise alignment of the resonator mode on the damage spot resulted in the laser operating with a specific vortex mode $LG_{0,1}$.

In 2018, Qiao et al. combined a simple two-mirror concave-planar cavity configuration with the defect mirror technique [114], as shown in Figure 3a. In this experiment, the cavity was composed of concave mirror M1, Nd:YAG crystal as gain medium pumped by laser diode (LD) and planar mirror as the output coupler (OC). The pump beam was collimated and focused by L1 and L2, respectively. In this way, the spot size and position can be optimized to match the on-demand laser mode. The laser mode selection mainly depends on the various round patterns inscribed on the OC by etching the coating layer using a Q-switched laser. The ratio (ε) between a round pattern radius (a) and TEM_{00} mode radius (ω_0) on the OC, corresponding to a specific $LG_{0,l}$ mode, can be theoretically calculated. On this basis, there were three ways to obtain an arbitrary topological charge: changing a by translating OC in the transvers plane to match the desired mode with corresponding round pattern, or changing ω_0 by adjusting the cavity length and slightly deviating the beam center by adjusting a round pattern. As a result, vortex beams with a topological charge up to 288 were generated. This fully proves the great potential of the defect mirror.

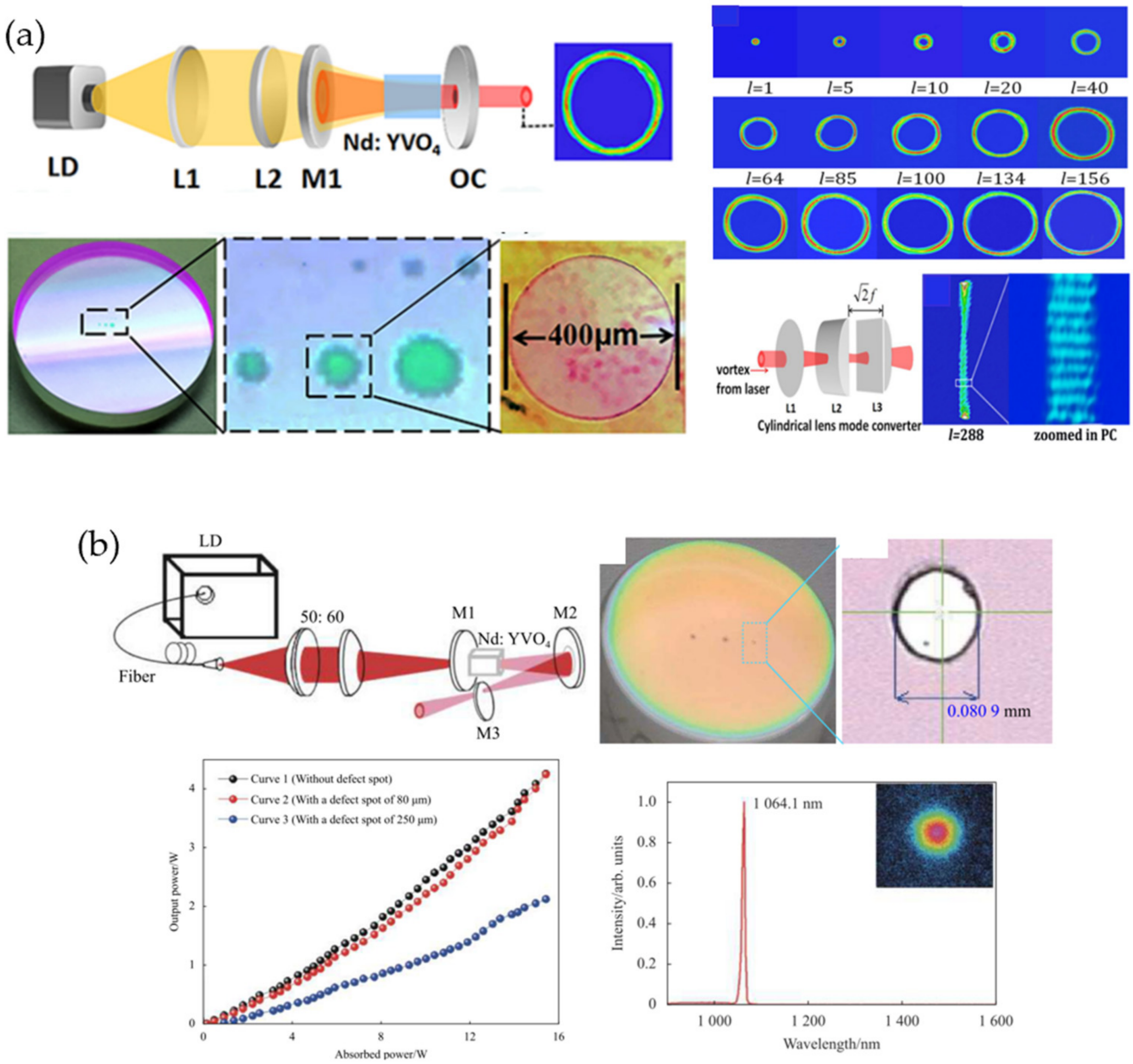

Figure 3. Vortex lasers using defected mirror. (**a**) Generation of high-charge optical vortices up to 288th order directly by laser cavity mirror etching. Reprinted with permission from [114] © 2018 The Authors. (**b**) A LD-end-pumped V-type Nd:YVO_4 vortex laser. Reprinted with permission from [115] © Infrared and Laser Engineering.

As shown above, from the current published research, the technique is mainly used in various two mirror linear cavities for laser generation in continuous-wave mode. However, in 2021, Xu et al. used a spot defect mirror in a diode-end-pumped Nd:YVO_4 laser with a V-shaped laser cavity [115], as shown in Figure 3b. The principle to achieve tunable topological charges was similar to the research mentioned above. Consequently, a high-order vortex laser with topological charges up to 11 and 13 was achieved. This research clearly indicates that the spot defect mirror technology can generate a high-order vortex laser directly in a structurally complicated laser resonator, providing references for Q-switched and mode-locked high-order vortex generation.

2.4. Intra-Cavity Modulation Devices

Inserting modulation devices into laser resonators is also an efficient way to generate vortex beams. Modulation devices include SPPs [116], diaphragms [117], acousto-optic modulators [118], etc. In recent years, the use of intra-cavity modulation devices to generate vector vortex beams has received extensive attention, and the use of QP, metasurfaces, and spatial light modulators (SLMs) can obtain tunable vector vortex beams.

2.4.1. Digital Laser

Generally, only a single laser mode can be generated without changing the structure of the laser cavity in a conventional laser. Yet, arbitrary laser mode can be selected in real-time by a digital laser, where a SLM loaded with different digital holograms plays an important role as the intra-cavity modulation device.

The digital laser was pioneered by S. Ngcobo et al. in 2013 [119]. The schematic of the digital laser is shown in Figure 4a. The laser was pumped by a LD, while a Nd:YAG crystal was employed as the gain medium. The L-shaped cavity was composed of the SLM, Brewster window (BW), high reflectivity (HR) mirror at an angle of 45°, Nd:YAG, and the OC. The phase-only reflective SLM was employed here as an end mirror of a solid-state laser. It can display digital holograms as pixelated grey-scale images, controlling by computer. Since the gray-scale colors ranging from white through black on SLM can graphically represent a full phase cycle, different phase modulation of reflected light at different positions can be obtained by loading specific digital holograms. In this way, structured beams of various modes including vortex beams were generated and no additional adjustment to the cavity is required. The different grayscale images loaded by SLM and their corresponding laser field of output laser modes in the digital laser are given in Figure 4b. It is proven that arbitrary laser modes including vortex beams can be generated this way by changing the digital holograms in real-time.

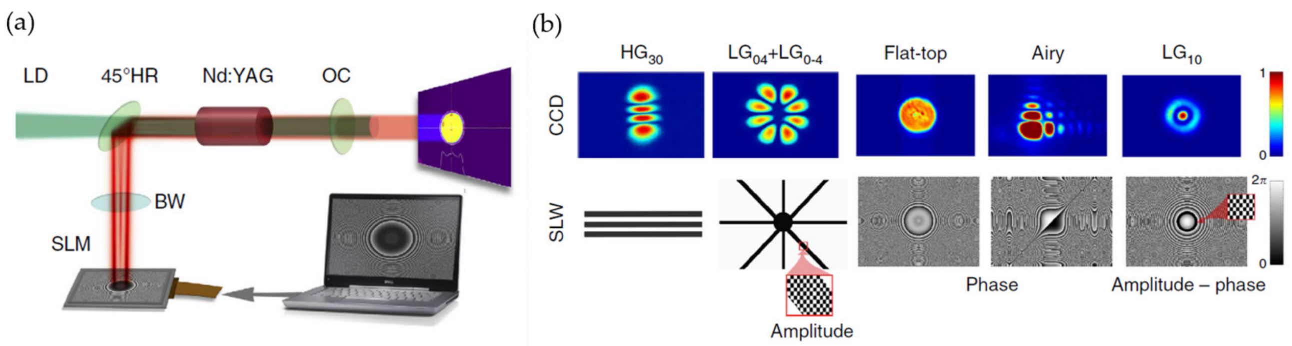

Figure 4. A digital laser for on-demand laser modes. (**a**)Schematic of the laser. (**b**)The greyscale images and corresponding laser field. Reprinted with permission from [119] © 2013 Macmillan Publishers Limited.

2.4.2. Q-Plate

Q-plate (QP) is a spatially varying waveplate made from liquid crystals. As a spin-orbital AM coupling device, it can be inserted into the cavity to generate vector vortex beams.

The earliest research began in 2016, when Naidoo et al. designed a mode-tunable vector vortex laser, where QPs and quarter-wave plates (QWPs) were introduced into the cavity [120]. It can be regarded as a scheme of geometric phase control while QWPs achieve polarization manipulation and QPs acts as a SAM–OAM converter. The transformation process of a pair of orthogonal circularly polarized beams passing through a QP with q-value of q can be described as $|L_l\rangle \longrightarrow |R_{\ell+2q}\rangle$ and $|R_\ell\rangle \longrightarrow |L_{\ell-2q}\rangle$, where $|L_l\rangle$ and $|R_\ell\rangle$ refer to left and right circularly polarized vortex beam with topological charges l and $-l$, $|R_{\ell+2q}\rangle$ and $|L_{\ell-2q}\rangle$ are interpreted similarly. These selection rules can be mathematically obtained by using the Jones matrix. To further illustrate, the schematic of the vector vortex laser is shown in Figure 5. The V-shaped cavity was composed of end mirrors, Nd:YAG as gain medium, polarizing beam splitter, a pair of QPs, a pair of QWPs, and a 45° mirror (FM) between two arms. The two arms structure was to ensure that the phase and polarization state can repeat the initial situation after one round-trip. As a result, the output modes which were also the repeating modes can be described as [120]

$$v_{\text{out}} = \cos\left(\frac{\Theta}{2}\right)\exp\left(-i\frac{\Phi}{2}\right)\left|L_{2q}\right\rangle + \sin\left(\frac{\Theta}{2}\right)\exp\left(i\frac{\Phi}{2}\right)\left|R_{-2q}\right\rangle, \tag{1}$$

where $\Theta = \pi/2 + 2\beta$ and $\Phi = 2\gamma - 2\beta$ where β and γ are the rotation angles of the QWP and QP, respectively, and $\left|L_{2q}\right\rangle$ and $\left|R_{-2q}\right\rangle$ refer to left and right circularly polarized vortex beam with topological charges $2q$ and $-2q$, respectively.

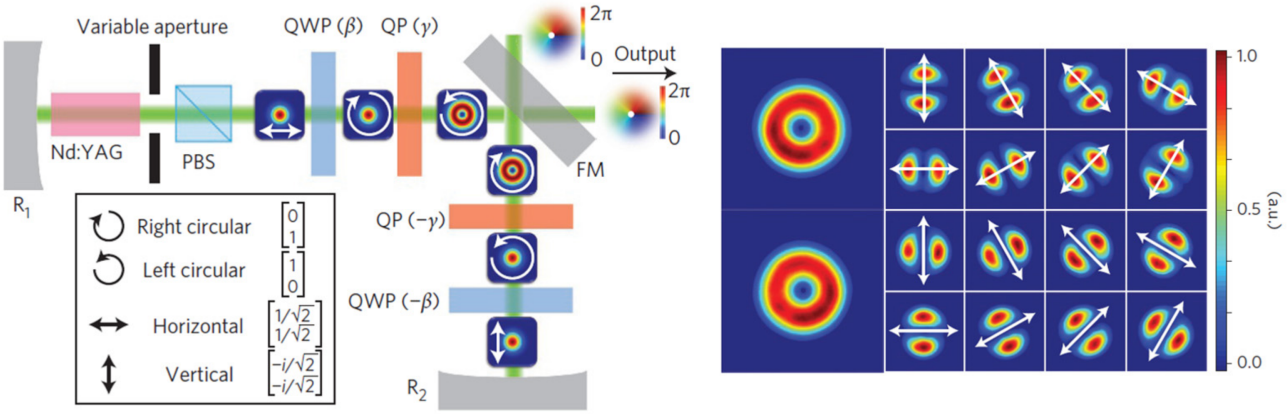

Figure 5. Generation of complex modes on HOP from a laser. Reprinted with permission from [120] © 2013 Macmillan Publishers Limited.

So, the output beams possessing polarization states and OAM states are obviously vector vortex beams, which can usually be described by a higher-order Poincaré sphere (HOP). The longitude coordinates of the vector vortex beam on the Poincaré sphere are jointly determined by the initial angle of the main axis of QP and QWP, and the latitude coordinates are determined by the initial angle of the main axis of QWP. The conversion of the fundamental mode Gaussian beam to the vortex beam can be realized by selecting the order of the QP, and then the main and fast axis angles of the QP and QWP can be rotated to control the mode of the vector vortex beam. To summarize, the spherical position of the vector vortex beams on the HOP can be flexibly adjusted by rotating the main and fast axis angles of the QP and QWP in the resonator without changing the structure of the cavity.

In the same way, Fan et al. designed a dual-beam pumped dual-channel OPO in 2020 [121], which placed a QWP and a QP in only one of the channels. The double output modes, including wavelength-tunable vector vortex beams and fundamental Gaussian beam, were generated. In the same years, our group reported that the mode-tunable generation of 1645 nm eye-safe band vector vortex beams can be achieved by inserting QWP and QP in the Er:YAG laser resonator [122].

In 2021, on the basis of the above work, our group proposed the simultaneous regulation of the transverse and longitudinal modes in the cavity [123], so as to generate single-frequency vector vortex beams at 1645 nm, as shown in Figure 6. The beam's transverse and longitudinal modes are tailored by the QP and the optical isolator (ISO) inside the cavity, respectively. By placing a non-reciprocal element ISO in the ring cavity, the spatial hole burning effect can be suppressed, and a single longitudinal mode output can be obtained. Meanwhile, the spin-orbital conversion device QP is employed to realize vector vortex beam generation. The total angular momentum (TAM) carried by the single-frequency vector vortex beam and the polarization distribution are determined by the q value and the main axis orientation of the QP, respectively.

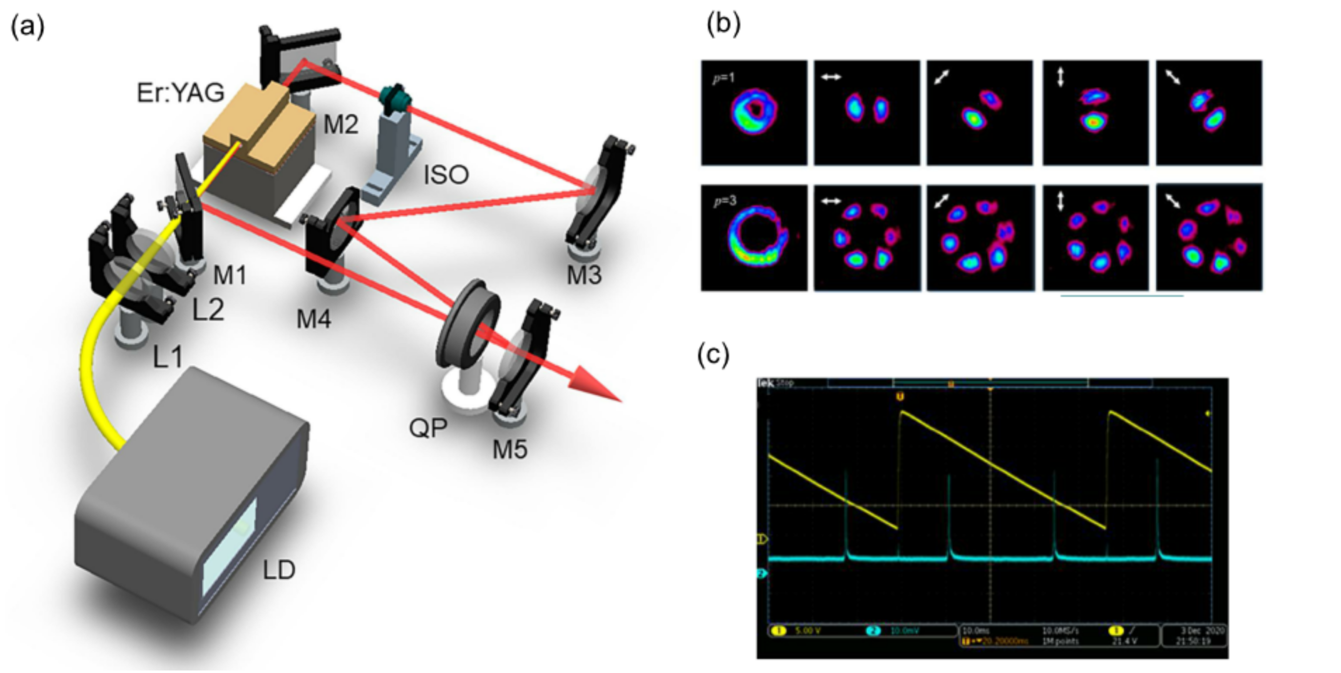

Figure 6. Simultaneous tailoring longitudinal and transverse mode inside an Er:YAG laser. (**a**) Schematic diagram of the laser; (**b**) Experimentally obtained intensity profiles of vectorial vortex beams when inserting q-plates with $q = 1/2$ (first row) and $q = 3/2$ (second row) in unidirectional operation before and after passing through a polarizer; (**c**) Scanning spectrum of the output single-longitudinal-mode 3rd order vectorial vortex beams in unidirectional operation. Reprinted with permission from [123] © 2021 Chinese Optics Letters.

2.4.3. Metasurface

The metasurfaces, consisting of subwavelength antenna arrays resulting in ultrathin thickness, is regarded as a two-dimensional surface. It can also act as a spin-orbital AM coupling device to achieve geometric phase control for the intra-cavity generation of vector vortex beams. A visible metasurface laser designed by H. Sroor et al. in 2020 showed a typical example [124].

According to their research, a new dielectric metasurface, the J-plate, has been made as a series of TiO_2 nanopillars with rectangular cross-sections designed directly in fused silica, as shown in Figure 7a. The amplitude and phase of an incident beam can be changed by inducing strong resonance of each unit structure. Compared with conventional metasurfaces, this new J-plate was designed to transform any two orthogonal polarization states into OAM states with arbitrary topological charge instead of only opposite topological charges. The J-plate was placed in the laser cavity and finally integrated to obtain a compact solid-state laser with nonlinear crystal (KTP) excited by an intra-cavity infrared pump, polarizer (Pol), and end mirrors, as shown in Figure 7b. To be more specific, the transformation process of a horizontally polarized state passing through the J-plate can be described as $|H,0\rangle \longrightarrow \cos(\theta)|H,l_1\rangle + \sin(\theta)|V,l_2\rangle$, where θ is the angle of the fast axis of the J-plate with respect to the horizontal. In this way, arbitrary AM control can be achieved in this laser by rotating the J-plate to change the fast axis angle. Compared to the previous method, more various modes can be generated in this laser. In addition to the ability of generating high-purity vector vortex beams of up to 100 orders OAM, the point is that various asymmetric vector vortex beams can also be obtained due to the properties of J-plate.

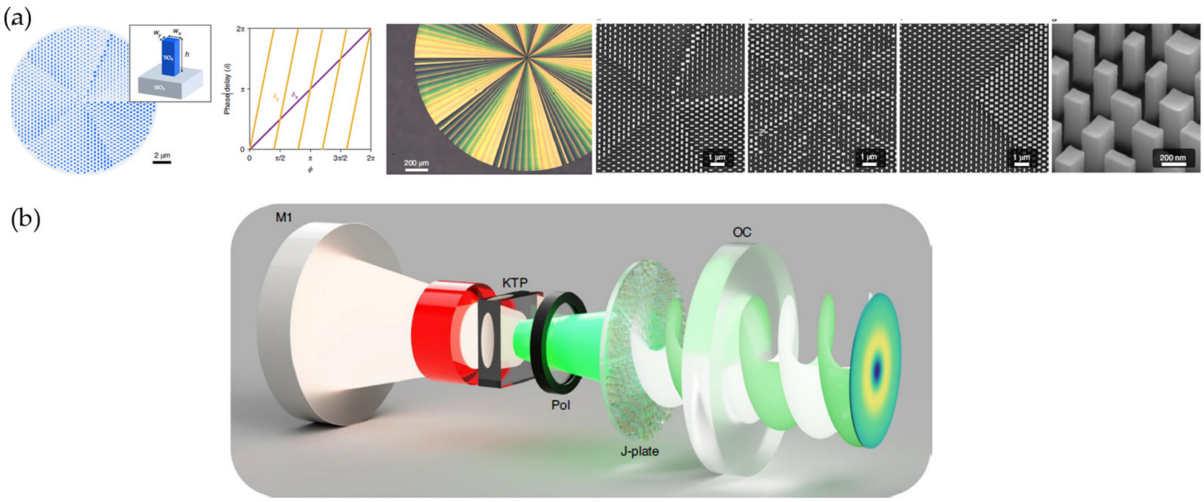

Figure 7. High-purity OAM states from a visible metasurface laser. (**a**) Design of new J-plate. (**b**) Schematic of the metasurface laser. Reprinted with permission from [124] © 2020, The Author(s), under exclusive license to Springer Nature Limited.

2.5. Others

Without the need for any special shaping or blocking elements, the direct generation of a vortex beam can be achieved within the laser by exploiting an undesired characteristic, namely the thermal lensing effect of the gain medium. This method is used to control the shape and power of pump beam by special means to control the thermal lens distribution inside the crystal due to thermal effects. This distribution can make the fundamental Gaussian mode beam with a smaller modal area have a larger energy distribution, which is more likely to produce a strong thermal lens effect. This resonator structure makes the fundamental mode exceed the stable state in the cavity to suppress the oscillation. Meanwhile, the vortex beam with a larger mode volume is oscillated in the cavity. In 2009, Chard et al. proposed the above theory and built a "bounced laser", as shown in Figure 8a [125], and Q-switched vortex pulses with the topological charge of 1 were obtained by adjusting the size of the pump beam and the rebound angle.

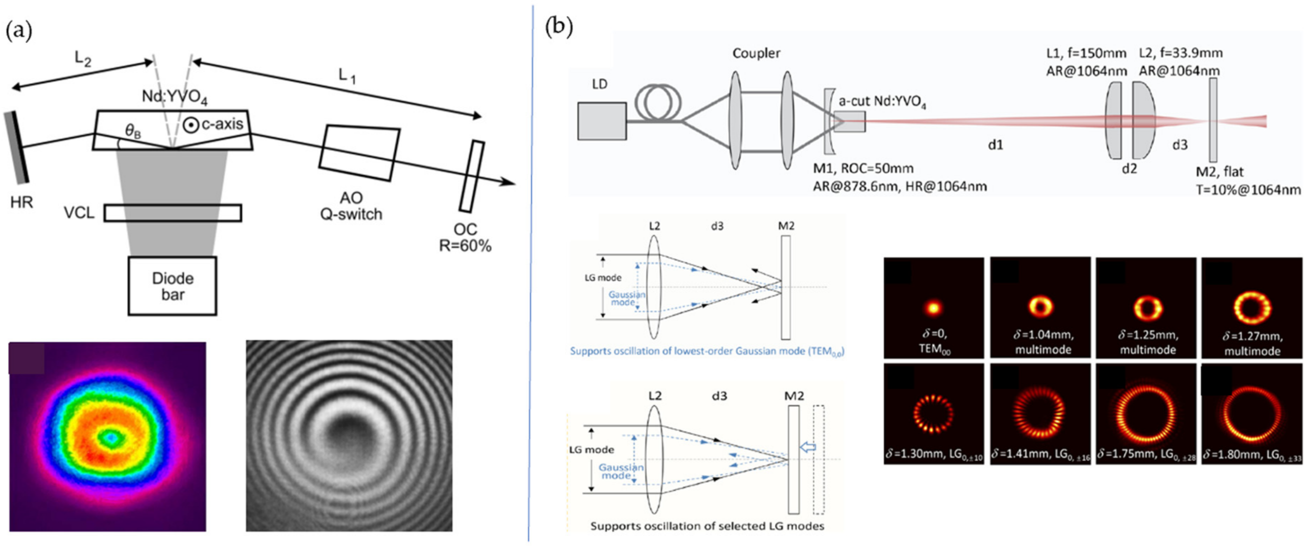

Figure 8. (**a**) Stigmatic Nd:YVO_4 bounce oscillator. Reprinted with permission from [125] © Springer-Verlag 2009; (**b**) LG mode selection by enhanced intracavity spherical aberration. Reprinted with permission from [126] © The Optical Society.

Another particularly interesting approach is the application of spherical aberration to facilitate the selection of intracavity modes with a hollow intensity profile. To generate a high-power laser beam that has a pure, high-order LG mode profile, it is necessary to ensure that the desired LG mode is well distinguished from other modes within the laser cavity. This can be achieved by enhancing the net gain difference between a desired LG mode and its neighboring modes. In 2021, Sheng et al. presented an LG mode laser based on enhanced spherical aberration (SA) [126]. The key to this approach is inducing strong SA within the cavity via expansion of the intra-cavity mode and having it incident on an intracavity, short-focal-length spherical lens, as shown in Figure 8b. This ensures that the optical path of the different orders of transverse modes with different spot sizes are spatially separated. Then, an end-pumped a-cut Nd:YVO_4 laser which delivers high-order scalar LG mode output with selectability was successfully demonstrated. The highest order hollow-intensity profile LG mode which could be selectively generated from this laser was $LG_{0, \pm 33.}$ Recently, on the basis of previous research, the same group further studied the characteristic of SA-induced cavity loss on LG mode selection, mainly focused on the influence caused by SA of different strength [127]. The high-order LG mode can be obtained by using long-focal-length spherical length to reduce the SA-induced losses on high order modes, which could even reach the angular index of ±95.

3. Conclusions

In this review, the fundamental principles and properties of vortex beams are briefly introduced. The ability to generate vortex beams with favorable performance is of great significance for their advanced applications. Compared with passive methods, we have summarized the approaches and recent advances in the field of intra-cavity vortex beam generation in solid-state lasers, especially vectorial vortex lasers, which can directly and flexibly generate vectorial vortex beams. The recent progress made in our work on an eye-safe vortex laser that exploits QPs and QWPs for vector vortex beam generation has been reviewed.

However, there are still many challenges concerning above intra-cavity generation. For example, the beam intensity distribution of the annular pump beam needs to be further improved in the later stage. Moreover, the thermal lens effect is only effective for the laser gain medium with obvious thermal effect and can easily lead to an unstable output and saturated output power. Besides, the current output beams of vortex lasers still have obvious shortcomings, such as low conversion efficiency, low output power, and low OAM order. In the future, there are still many technical challenges to be faced and addressed.

Funding: National Natural Science Foundation of China (11834001, 61905012); National Defense Basic Scientific Research Program of China (JCKY2020602C007); National Postdoctoral Program for Innovative Talents (BX20190036); Beijing Institute of Technology Research Fund Program for Young Scholars.

Institutional Review Board Statement: Not applicable.

Informed Consent Statement: Not applicable.

Data Availability Statement: Not applicable.

Conflicts of Interest: The authors declare no conflict of interest.

References

1. Forbes, A.; Dudley, A.; McLaren, M. Creation and detection of optical modes with spatial light modulators. *Adv. Opt. Photonics* **2016**, *8*, 200–227.
2. Strickland, D.; Mourou, G. Compression of amplified chirped optical pulses. *Opt. Commun.* **1985**, *55*, 447–449.
3. Fu, S.Y.; Han, X.; Song, R.; Huang, L.; Gao, C.Q. Generating a 64 × 64 beam lattice by geometric phase modulation from arbitrary incident polarizations. *Opt. Lett.* **2020**, *45*, 6330–6333. [PubMed]
4. Fu, S.Y.; Wang, T.L.; Zhang, Z.Y.; Zhai, Y.W.; Gao, C.Q. Selective acquisition of multiple states on hybrid Poincare sphere. *Appl. Phys. Lett.* **2017**, *110*, 191102.

5. Fu, S.Y.; Gao, C.Q.; Wang, T.L.; Zhang, S.K.; Zhai, Y.W. Simultaneous generation of multiple perfect polarization vortices with selective spatial states in various diffraction orders. *Opt. Lett.* **2016**, *41*, 5454–5457.
6. Chang, G.Q.; Wei, Z.Y. Ultrafast Fiber Lasers: An Expanding Versatile Toolbox. *Iscience* **2020**, *23*, 101101.
7. Liu, W.J.; Liu, M.L.; Chen, X.; Shen, T.; Lei, M.; Guo, J.G.; Deng, H.X.; Zhang, W.; Dai, C.Q.; Zhang, X.F.; et al. Ultrafast photonics of two dimensional AuTe2Se4/3 in fiber lasers. *Commun. Phys.* **2020**, *3*, 15.
8. Gori, F.; Guattari, G.; Padovani, C. Bessel-Gauss beams. *Opt. Commun.* **1987**, *64*, 491–495.
9. Efremidis, N.K.; Chen, Z.G.; Segev, M.; Christodoulides, D.N. Airy beams and accelerating waves: An overview of recent advances. *Optica* **2019**, *6*, 686–701.
10. Zhuang, J.L.; Zhang, L.P.; Deng, D.M. Tight-focusing properties of linearly polarized circular Airy Gaussian vortex beam. *Opt. Lett.* **2020**, *45*, 296–299.
11. Zhan, Q.W. Cylindrical vector beams: From mathematical concepts to applications. *Adv. Opt. Photonics* **2009**, *1*, 828–891.
12. Shen, Y.J.; Yang, X.L.; Naidoo, D.; Fu, X.; Forbes, A. Structured ray-wave vector vortex beams in multiple degrees of freedom from a laser. *Optica* **2020**, *7*, 820–831.
13. Wang, Z.Y.; Shen, Y.J.; Naidoo, D.; Fu, X.; Forbes, A. Astigmatic hybrid SU(2) vector vortex beams: Towards versatile structures in longitudinally variant polarized optics. *Opt. Express* **2021**, *29*, 315–329. [PubMed]
14. Allen, L.; Beijersbergen, M.W.; Spreeuw, R.J.C.; Woerdman, J.P. Orbital angular-momentum of light and the transformation of Laguerre-Gaussian laser modes. *Phys. Rev. A* **1992**, *45*, 8185–8189. [PubMed]
15. Bai, Y.; Lv, H.; Fu, X.; Yang, Y. Vortex beam: Generation and detection of orbital angular momentum. *Chin. Opt. Lett.* **2022**, *20*, 012601.
16. Zhou, H.; Yang, J.Q.; Gao, C.Q.; Fu, S.Y. High-efficiency, broadband all-dielectric transmission metasurface for optical vortex generation. *Opt. Mater. Express* **2019**, *9*, 2806.
17. Zhang, J.; Sun, C.Z.; Xiong, B.; Wang, J.; Hao, Z.B.; Wang, L.; Han, Y.J.; Li, H.T.; Luo, Y.; Xiao, Y.; et al. An InP-based vortex beam emitter with monolithically integrated laser. *Nat. Commun.* **2018**, *9*, 1–6.
18. Cai, X.L.; Wang, J.W.; Strain, M.J.; Johnson-Morris, B.; Zhu, J.B.; Sorel, M.; O'Brien, J.L.; Thompson, M.G.; Yu, S.T. Integrated Compact Optical Vortex Beam Emitters. *Science* **2012**, *338*, 363–366.
19. Yang, Y.; Zhao, Q.; Liu, L.; Liu, Y.; Rosales-Guzman, C.; Qiu, C.-W. Manipulation of Orbital-Angular-Momentum Spectrum Using Pinhole Plates. *Phys. Rev. Appl.* **2019**, *12*, 064007.
20. Zeng, R.; Zhao, Q.; Shen, Y.; Liu, Y.; Yang, Y. Structural stability of open vortex beams. *Appl. Phys. Lett.* **2021**, *119*, 171105.
21. Wang, J.; Yang, J.Y.; Fazal, I.M.; Ahmed, N.; Yan, Y.; Huang, H.; Ren, Y.; Yue, Y.; Dolinar, S.; Tur, M.; et al. Terabit free-space data transmission employing orbital angular momentum multiplexing. *Nat. Photonics* **2012**, *6*, 488–496.
22. Bozinovic, N.; Yue, Y.; Ren, Y.; Tur, M.; Kristensen, P.; Huang, H.; Willner, A.E.; Ramachandran, S. Terabit-Scale Orbital Angular Momentum Mode Division Multiplexing in Fibers. *Science* **2013**, *340*, 1545–1548. [PubMed]
23. Yu, S. Potentials and challenges of using orbital angular momentum communications in optical interconnects. *Opt. Express* **2015**, *23*, 3075–3087. [PubMed]
24. Willner, A.E.; Huang, H.; Yan, Y.; Ren, Y.; Ahmed, N.; Xie, G.; Bao, C.; Li, L.; Cao, Y.; Zhao, Z.; et al. Optical communications using orbital angular momentum beams. *Adv. Opt. Photonics* **2015**, *7*, 66–106.
25. Wang, J. Advances in communications using optical vortices. *Photonics Res.* **2016**, *4*, B14–B28.
26. Fu, S.; Zhai, Y.; Zhou, H.; Zhang, J.; Yin, C.; Gao, C. Demonstration of high-dimensional free-space data coding/decoding through multi-ring optical vortices. *Chin. Opt. Lett.* **2019**, *17*, 080602.
27. Fu, S.; Zhai, Y.; Zhou, H.; Zhang, J.; Wang, T.; Yin, C.; Gao, C. Demonstration of free-space one-to-many multicasting link from orbital angular momentum encoding. *Opt. Lett.* **2019**, *44*, 4753–4756.
28. Fu, S.; Zhai, Y.; Zhou, H.; Zhang, J.; Wang, T.; Liu, X.; Gao, C. Experimental demonstration of free-space multi-state orbital angular momentum shift keying. *Opt. Express* **2019**, *27*, 33111–33119.
29. Lavery, M.P.J.; Speirits, F.C.; Barnett, S.M.; Padgett, M.J. Detection of a Spinning Object Using Light's Orbital Angular Momentum. *Science* **2013**, *341*, 537–540.
30. Lavery, M.P.J.; Barnett, S.M.; Speirits, F.C.; Padgett, M.J. Observation of the rotational Doppler shift of a white-light, orbital-angular-momentum-carrying beam backscattered from a rotating body. *Optica* **2014**, *41*, 2549–2552.
31. Fu, S.; Wang, T.; Zhang, Z.; Zhai, Y.; Gao, C. Non-diffractive Bessel-Gauss beams for the detection of rotating object free of obstructions. *Opt. Express* **2017**, *25*, 20098–20108. [PubMed]
32. Fang, L.; Padgett, M.J.; Wang, J. Sharing a Common Origin Between the Rotational and Linear Doppler Effects. *Laser Photonics Rev.* **2017**, *11*, 1700183.
33. Zhang, W.; Gao, J.; Zhang, D.; He, Y.; Xu, T.; Fickler, R.; Chen, L. Free-Space Remote Sensing of Rotation at the Photon-Counting Level. *Phys. Rev. Appl.* **2018**, *10*, 044014.
34. Zhai, Y.; Fu, S.; Yin, C.; Zhou, H.; Gao, C. Detection of angular acceleration based on optical rotational Doppler effect. *Opt. Express* **2019**, *27*, 15518–15527. [PubMed]
35. Qiu, S.; Liu, T.; Ren, Y.; Li, Z.; Wang, C.; Shao, Q. Detection of spinning objects at oblique light incidence using the optical rotational Doppler effect. *Opt. Express* **2019**, *27*, 24781–24792.
36. Zhai, Y.; Fu, S.; Zhang, J.; Lv, Y.; Zhou, H.; Gao, C. Remote detection of a rotator based on rotational Doppler effect. *Appl. Phys. Express* **2020**, *13*, 022012.

37. Padgett, M.; Bowman, R. Tweezers with a twist. *Nat. Photonics* **2011**, *5*, 343–348.
38. Chen, M.; Mazilu, M.; Arita, Y.; Wright, E.M.; Dholakia, K. Dynamics of microparticles trapped in a perfect vortex beam. *Opt. Lett.* **2013**, *38*, 4919–4922.
39. Gecevicius, M.; Drevinskas, R.; Beresna, M.; Kazansky, P.G. Single beam optical vortex tweezers with tunable orbital angular momentum. *Appl. Phys. Lett.* **2014**, *104*, 231110.
40. Liang, Y.; Yao, B.; Ma, B.; Lei, M.; Yan, S.; Yu, X. Holographic Optical Trapping and Manipulation Based on Phase-only Liquid-Crystal Spatial Light Modulator. *Acta Opt. Sin.* **2016**, *36*, 0309001–0309007.
41. Yang, Y.; Ren, Y.-X.; Chen, M.; Arita, Y.; Rosales-Guzman, C. Optical trapping with structured light: A review. *Adv. Photonics* **2021**, *3*, 034001.
42. Rosales-Guzman, C.; Ndagano, B.; Forbes, A. A review of complex vector light fields and their applications. *J. Opt.* **2018**, *20*, 123001.
43. Fu, S.Y.; Hai, L.; Song, R.; Gao, C.Q.; Zhang, X.D. Representation of total angular momentum states of beams through a four-parameter notation. *New J. Phys.* **2021**, *23*, 083015.
44. Kagalwala, K.H.; Di Giuseppe, G.; Abouraddy, A.F.; Saleh, B.E.A. Bell's measure in classical optical coherence. *Nat. Phys.* **2013**, *7*, 72–78.
45. Ndagano, B.; Bruening, R.; McLaren, M.; Duparre, M.; Forbes, A. Fiber propagation of vector modes. *Opt. Express* **2015**, *23*, 17330–17336.
46. Berg-Johansen, S.; Toeppel, F.; Stiller, B.; Banzer, P.; Ornigotti, M.; Giacobino, E.; Leuchs, G.; Aiello, A.; Marquardt, C. Classically entangled optical beams for high-speed kinematic sensing. *Optica* **2015**, *2*, 864–868.
47. Rafsanjani, S.M.H.; Mirhosseini, M.; Magana-Loaiza, O.S.; Boyd, R.W. State transfer based on classical nonseparability. *Phys. Rev. A* **2015**, *92*, 023827.
48. Harris, J.; Grillo, V.; Mafakheri, E.; Gazzadi, G.C.; Frabboni, S.; Boyd, R.W.; Karimi, E. Structured quantum waves. *Nat. Phys.* **2015**, *11*, 629–634.
49. Bandyopadhyay, P.; Basu, B.; Chowdhury, D. Relativistic Electron Vortex Beams in a Laser Field. *Phys. Rev. Lett.* **2015**, *115*, 194801.
50. Niziev, V.G.; Nesterov, A.V. Influence of beam polarization on laser cutting efficiency. *J. Phys. D* **1999**, *32*, 1455–1461.
51. Meier, M.; Romano, V.; Feurer, T. Material processing with pulsed radially and azimuthally polarized laser radiation. *Appl. Phys. A* **2007**, *86*, 329–334.
52. Zhao, W.Q.; Tang, F.; Qiu, L.R.; Liu, D.L. Research status and application on the focusing properties of cylindrical vector beams. *Acta Phys. Sin.* **2013**, *62*, 054201.
53. Zhou, Z.; Tan, Q.; Jin, G. Surface plasmon interference formed by tightly focused higher polarization order axially symmetric polarized beams. *Chin. Opt. Lett.* **2010**, *8*, 1178–1181.
54. Wang, X.; Nie, Z.; Liang, Y.; Wang, J.; Li, T.; Jia, B. Recent advances on optical vortex generation. *Nanophononics* **2018**, *7*, 1533–1556.
55. Forbes, A. Structured Light from Lasers. *Laser Photonics Rev.* **2019**, *13*, 1900140.
56. Shen, Y.; Wang, X.; Xie, Z.; Min, C.; Fu, X.; Liu, Q.; Gong, M.; Yuan, X. Optical vortices 30 years on: OAM manipulation from topological charge to multiple singularities. *Light Sci. Appl* **2019**, *8*, 1–29.
57. Liu, Q.; Pan, J.; Wan, Z.; Shen, Y.; Zhang, H.; Fu, X.; Gong, M. Generation Methods for Complex Vortex Structured Light Field. *Chin. J. Lasers* **2020**, *47*, 0500006.
58. Beijersbergen, M.W.; Allen, L.; Vanderveen, H.; Woerdman, J.P. Astigmatic laser mode converters and transfer of orbital angular-momentum. *Opt. Commun.* **1993**, *96*, 123–132.
59. Malyutin, A.A.; Ilyukhin, V.A. Generation of high-order Hermite-Gaussian modes in a flashlamp-pumped neodymium phosphate glass laser and their conversion to Laguerre-Gaussian modes. *Quantum Electron.* **2007**, *37*, 181–186.
60. Beijersbergen, M.W.; Coerwinkel, R.P.C.; Kristensen, M.; Woerdman, J.P. Helical-wave-front laser beams produced with a spiral phaseplate. *Opt. Commun.* **1994**, *112*, 321–327.
61. Turnbull, G.A.; Robertson, D.A.; Smith, G.M.; Allen, L.; Padgett, M.J. Generation of free-space Laguerre-Gaussian modes at millimetre-wave frequencies by use of a spiral phaseplate. *Opt. Commun.* **1996**, *127*, 183–188.
62. Xin, J.; Dai, K.; Zhong, L.; Na, Q.; Gao, C. Generation of optical vortices by using spiral phase plates made of polarization dependent devices. *Opt. Lett.* **2014**, *39*, 1984–1987. [PubMed]
63. Xiong, M.; Ding, P.; Pu, J. Analysis on the Beam Characteristic of Gaussian Beam Passing Multi-Level Spiral Phase Plate. *Laser Optoelectron. Prog.* **2015**, *52*, 081902.
64. Guo, M.; Zeng, J.; Li, J. Generation and Interference of Vortex Beam Based on Spiral Phase Plate. *Laser Optoelectron. Prog.* **2016**, *53*, 092602.
65. Heckenberg, N.R.; McDuff, R.; Smith, C.P.; White, A.G. Generation of optical-phase singularities by computer-generated holograms. *Opt. Lett.* **1992**, *17*, 221–223.
66. Davis, J.A.; McNamara, D.E.; Cottrell, D.M.; Campos, J. Image processing with the radial Hilbert transform: Theory and experiments. *Opt. Lett.* **2000**, *25*, 99–101.
67. Guo, C.S.; Liu, X.; Ren, X.Y.; Wang, H.T. Optimal annular computer-generated holograms for the generation of optical vortices. *J. Opt. Soc. Am. A* **2005**, *22*, 385–390.
68. Sun, J.; Wang, X.; Xu, T.; Kudyshev, Z.A.; Cartwright, A.N.; Litchinitser, N.M. Spinning Light on the Nanoscale. *Nano Lett.* **2014**, *14*, 2726–2729.

69. Mehmood, M.Q.; Mei, S.; Hussain, S.; Huang, K.; Siew, S.Y.; Zhang, L.; Zhang, T.; Ling, X.; Liu, H.; Teng, J.; et al. Visible-Frequency Metasurface for Structuring and Spatially Multiplexing Optical Vortices. *Adv. Mater.* **2016**, *28*, 2533.
70. Devlin, R.C.; Ambrosio, A.; Rubin, N.A.; Mueller, J.P.B.; Capasso, F. Arbitrary spin-to-orbital angular momentum conversion of light. *Science* **2017**, *358*, 896–900.
71. Zhang, Y.; Liu, W.; Gao, J.; Yang, X. Generating Focused 3D Perfect Vortex Beams by Plasmonic Metasurfaces. *Adv. Opt. Mater.* **2018**, *6*, 1701228.
72. Ren, Y.X.; Li, M.; Huang, K.; Wu, J.G.; Gao, H.F.; Wang, Z.Q.; Li, Y.-M. Experimental generation of Laguerre-Gaussian beam using digital micromirror device. *Appl. Opt.* **2010**, *49*, 1838–1844. [PubMed]
73. Mirhosseini, M.; Magana-Loaiza, O.S.; Chen, C.; Rodenburg, B.; Malik, M.; Boyd, R.W. Rapid generation of light beams carrying orbital angular momentum. *Opt. Express* **2013**, *21*, 30196–30203. [PubMed]
74. Chen, Y.; Fang, Z.X.; Ren, Y.X.; Gong, L.; Lu, R.D. Generation and characterization of a perfect vortex beam with a large topological charge through a digital micromirror device. *Appl. Opt.* **2015**, *54*, 8030–8035.
75. Ji, W.; Lee, C.H.; Chen, P.; Hu, W.; Ming, Y.; Zhang, L.; Lin, T.H.; Chigrinov, V.; Lu, Y.-Q. Meta-q-plate for complex beam shaping. *Sci. Rep.* **2016**, *6*, 25528.
76. Fu, S.; Gao, C.; Shi, Y.; Dai, K.; Zhong, L.; Zhang, S. Generating polarization vortices by using helical beams and a Twyman Green interferometer. *Opt. Lett.* **2015**, *40*, 1775–1778.
77. Wang, T.; Fu, S.; Zhang, S.; Gao, C.; He, F. A Sagnac-like interferometer for the generation of vector beams. *Appl. Phys. B* **2016**, *122*, 231.
78. Fu, S.; Wang, T.; Gao, C. Generating perfect polarization vortices through encoding liquid-crystal display devices. *Appl. Opt.* **2016**, *55*, 6501–6505.
79. Fu, S.; Wang, T.; Gao, C. Perfect optical vortex array with controllable diffraction order and topological charge: Erratum. *J. Opt. Soc. Am. A* **2016**, *33*, 2076.
80. Fu, S.; Zhai, Y.; Wang, T.; Yin, C.; Gao, C. Tailoring arbitrary hybrid Poincare beams through a single hologram. *Appl. Phys. Lett.* **2017**, *111*, 211101.
81. Mao, D.; Zheng, Y.; Zeng, C.; Lu, H.; Wang, C.; Zhang, H.; Zhang, W.; Mei, T.; Zhao, J. Generation of polarization and phase singular beams in fibers and fiber lasers. *Adv. Photonics* **2021**, *3*, 014002.
82. Fu, P.; Ni, P.N.; Wang, Q.H.; Liu, Y.F.; Wu, B.; Chen, P.P.; Kan, Q.; Wang, S.P.; Chen, H.D.; Xu, C.; et al. Multichannel Generations of Orbital Angular Momentum Modes with On-Demand Characteristics on a Chip. *Adv. Opt. Mater.* **2021**, *9*, 2101308.
83. Prati, F.; Tissoni, G.; SanMiguel, M.; Abraham, N.B. Vector vortices and polarization state of low-order transverse modes in a VCSEL. *Opt. Commun.* **1997**, *143*, 133–146.
84. Jimenez-Garcia, J.; Rodriguez, P.; Guillet, T.; Ackemann, T. Spontaneous Formation of Vector Vortex Beams in Vertical-Cavity Surface-Emitting Lasers with Feedback. *Phys. Rev. Lett.* **2017**, *119*, 113902.
85. Wang, K.; Gao, C.; Lin, Z.; Wang, Q.; Gao, M.; Huang, S.; Chen, C. 1645 nm coherent Doppler wind lidar with a single-frequency Er:YAG laser. *Opt. Express* **2020**, *28*, 14694–14704.
86. Stephan, C.; Alpers, M.; Millet, B.; Ehret, G.; Flamant, P.; Deniel, C. MERLIN—A space-based methane monitor. In Proceedings of the Conference on Lidar Remote Sensing for Environmental Monitoring XII, San Diego, CA, USA, 21–22 August 2011.
87. Chen, Y.F.; Lan, Y.P.; Wang, S.C. Generation of Laguerre-Gaussian modes in fiber-coupled laser diode end-pumped lasers. *Appl. Phys. B* **2001**, *72*, 167–170.
88. Zhao, Y.; Liu, Q.; Zhou, W.; Shen, D. ~1 mJ pulsed vortex laser at 1645 nm with well-defined helicity. *Opt. Express* **2016**, *24*, 15596–15602.
89. Liu, Q.; Zhao, Y.; Zhou, W.; Shen, D. Vortex operation in Er:LuYAG crystal laser at similar to 1.6 μm. *Opt. Mater.* **2017**, *71*, 31–34.
90. Liu, Q.; Zhao, Y.; Ding, M.; Yao, W.; Fan, X.; Shen, D. Wavelength-and OAM-tunable vortex laser with a reflective volume Bragg grating. *Opt. Express* **2017**, *25*, 23312–23319.
91. Liu, Q.; Zhao, Y.; Zhou, W.; Zhang, J.; Wang, L.; Yao, W.; Shen, D. Control of Vortex Helicity With a Quarter-Wave Plate in an Er:YAG Ceramic Solid State Laser. *IEEE Photon. J.* **2017**, *9*, 1–8.
92. Fang, Z.; Yao, Y.; Xia, K.; Li, J. Actively Q-switched and vortex Nd:YAG laser. *Opt. Commun.* **2015**, *347*, 59–63.
93. Fang, Z.; Yao, Y.; Xia, K.; Li, J. Simple Nd:YAG laser generates vector and vortex beam. *Chin. Opt. Lett.* **2015**, *13*, 031405.
94. Kim, J.W. High-power laser operation of the first-order Laguerre-Gaussian (LG_{01}) mode in a diode-laser-pumped Nd:YAG laser. *J. Korean Phys. Soc.* **2012**, *61*, 739–743.
95. Kim, J.W.; Clarkson, W.A. Selective generation of Laguerre-Gaussian (LG_{0n}) mode output in a diode-laser pumped Nd:YAG laser. *Opt. Commun.* **2013**, *296*, 109–112.
96. Kim, D.J.; Kim, J.W.; Clarkson, W.A. Q-switched Nd:YAG optical vortex lasers. *Opt. Express* **2013**, *21*, 29449–29454.
97. Lin, D.; Daniel, J.M.O.; Clarkson, W.A. Controlling the handedness of directly excited Laguerre-Gaussian modes in a solid-state laser. *Opt. Lett.* **2014**, *39*, 3903–3906.
98. Lu, J.; Lin, H.; Zhang, G.; Li, B.; Zhang, L.; Lin, Z.; Chen, Y.F.; Petrov, V.; Chen, W. Direct generation of an optical vortex beam from a diode-pumped Yb:$MgWO_4$ laser. *Laser Phys. Lett.* **2017**, *14*, 085807.
99. Bisson, J.E.; Senatsky, Y.; Ueda, K.I. Generation of Laguerre-Gaussian modes in Nd: YAG laser using diffractive optical pumping. *Laser Phys. Lett.* **2005**, *2*, 327–333.

100. Li, J.; Yao, Y.; Yu, J.; Xia, K.; Zhou, C. Efficient Vortex Laser with Annular Pumping Formed by Circle Dammann Grating. *IEEE Photon.* **2016**, *28*, 473–476.
101. Schepers, F.; Bexter, T.; Hellwig, T.; Fallnich, C. DMD-Based Excitation of Transverse Laser Modes by Spatial Pump Beam Shaping. In Conference on Lasers and Electro-Optics Europe/European Quantum Electronics Conference (CLEO/Europe-EQEC), Munich, Germany, 23–27 June; 2019.
102. Wei, M.D.; Lai, Y.-S.; Chang, K.C. Generation of a radially polarized laser beam in a single microchip Nd:YVO4 laser. *Opt. Lett.* **2013**, *38*, 2443–2445.
103. He, H.S.; Chen, Z.; Dong, J. Direct generation of vector vortex beams with switchable radial and azimuthal polarizations in a monolithic Nd:YAG microchip laser. *Appl. Phys. Express* **2017**, *10*, 052701.
104. Chen, Y.F.; Huang, T.M.; Kao, C.F.; Wang, C.L.; Wang, S.C. Generation of Hermite-Gaussian modes in fiber-coupled laser-diode end-pumped lasers. *IEEE J. Quantum Electron.* **1997**, *33*, 1025–1031.
105. Laabs, H.; Ozygus, B. Excitation of Hermite Gaussian modes in end-pumped solid-state lasers via off-axis pumping. *Opt. Laser Technol.* **1996**, *28*, 213–214.
106. Chu, S.C.; Ohtomo, T.; Otsuka, K. Generation of doughnutlike vortex beam with tunable orbital angular momentum from lasers with controlled Hermite-Gaussian modes. *Appl. Opt.* **2008**, *47*, 2583–2591.
107. Huang, X.; Xu, B.; Cui, S.; Xu, H.; Cai, Z.; Chen, L. Direct Generation of Vortex Laser by Rotating Induced Off-Axis Pumping. *IEEE J. Sel. Top. Quantum Electron.* **2018**, *24*, 1–6.
108. Wang, S.; Zhang, S.L.; Qiao, H.C.; Li, P.; Hao, M.H.; Yang, H.M.; Xie, J.; Feng, G.Y.; Zhou, S.H. Direct generation of vortex beams from a double-end polarized pumped Yb:KYW laser. *Opt. Express* **2018**, *26*, 26925–26932.
109. Lin, G.; Cao, Y.; Lu, Z.; Chembo, Y.K. Spontaneous generation of orbital angular momentum crystals using a monolithic Nd:YAG nonplanar ring laser. *Opt. Lett.* **2019**, *44*, 203–206.
110. Liu, J.; Lin, J.; Chen, X.; Yu, Y.; Wu, C.; Jin, G. A 1.9 km Tm: YLF external cavity mode conversion vortex laser based on LD off-axis pump. *Opt. Commun.* **2021**, *482*, 126596.
111. Shen, Y.; Meng, Y.; Fu, X.; Gong, M. Wavelength-tunable Hermite-Gaussian modes and an orbital-angular-momentum-tunable vortex beam in a dual-off-axis pumped Yb:CALGO laser. *Opt. Lett.* **2018**, *43*, 291–294.
112. Ito, A.; Kozawa, Y.; Sato, S. Generation of hollow scalar and vector beams using a spot-defect mirror. *J. Opt. Soc. Am. A* **2010**, *27*, 2072–2077.
113. Lee, A.J.; Omatsu, T.; Pask, H.M. Direct generation of a first-Stokes vortex laser beam from a self-Raman laser. *Opt. Express* **2013**, *21*, 12401–12408. [PubMed]
114. Qiao, Z.; Xie, G.; Wu, Y.; Yuan, P.; Ma, J.; Qian, L.; Fan, D. Generating High-Charge Optical Vortices Directly from Laser Up to 288th Order. *Laser Photonics Rev.* **2018**, *12*, 1800019.
115. Zhou, L.; Feng, K.; Wang, D.; Xu, B. Research on direct generation of high-power and high-order vortex lasers using defect-mirror technology. *Infrared Laser Eng.* **2021**, *50*, 20210408.
116. Oron, R.; Danziger, Y.; Davidson, N.; Friesem, A.A.; Hasman, E. Laser mode discrimination with intra-cavity spiral phase elements. *Opt. Commun.* **1999**, *169*, 115–121.
117. Kim, D.J.; Kim, J.W. High-power TEM00 and Laguerre-Gaussian mode generation in double resonator configuration. *Appl. Phys. B* **2015**, *121*, 401–405.
118. Kim, D.J.; Mackenzie, J.I.; Kim, J.W. Adaptable beam profiles from a dual-cavity Nd:YAG laser. *Opt. Lett.* **2016**, *41*, 1740–1743.
119. Ngcobo, S.; Litvin, I.; Burger, L.; Forbes, A. A digital laser for on-demand laser modes. *Nat. Commun.* **2013**, *4*, 1–6.
120. Naidoo, D.; Roux, F.S.; Dudley, A.; Litvin, I.; Piccirillo, B.; Marrucci, L.; Forbes, A. Controlled generation of higher-order Poincare sphere beams from a laser. *Nat. Photonics* **2016**, *10*, 327.
121. Fan, J.; Zhao, J.; Shi, L.; Xiao, N.; Hu, M. Two-channel, dual-beam-mode, wavelength-tunable femtosecond optical parametric oscillator. *Adv. Photonics* **2020**, *2*, 045001.
122. Song, R.; Gao, C.; Zhou, H.; Fu, S. Resonantly pumped Er:YAG vector laser with selective polarization states at 1.6 µm. *Opt. Lett.* **2020**, *45*, 4626–4629.
123. Song, R.; Liu, X.; Fu, S.; Gao, C. Simultaneous tailoring of longitudinal and transverse mode inside an Er:YAG laser. *Chin. Opt. Lett.* **2021**, *19*, 111404.
124. Sroor, H.; Huang, Y.W.; Sephton, B.; Naidoo, D.; Valles, A.; Ginis, V.; Qiu, C.W.; Ambrosio, A.; Capasso, F.; Forbes, A. High-purity orbital angular momentum states from a visible metasurface laser. *Nat. Photonics* **2020**, *14*, 498.
125. Chard, S.P.; Shardlow, P.C.; Damzen, M.J. High-power non-astigmatic TEM00 and vortex mode generation in a compact bounce laser design. *Appl. Phys. B* **2009**, *97*, 275–280.
126. Wang, M.; Ma, Y.; Sheng, Q.; He, X.; Liu, J.; Shi, W.; Yao, J.; Omatsu, T. Laguerre-Gaussian beam generation via enhanced intracavity spherical aberration. *Opt. Express* **2021**, *29*, 27783–27790. [PubMed]
127. Sheng, Q.; Wang, A.H.; Ma, Y.Y.; Wang, S.J.; Wang, M.; Shi, Z.; Liu, J.J.; Fu, S.J.; Shi, W.; Yao, J.Q.; et al. Intracavity spherical aberration for selective generation of single-transverse-mode Laguerre-Gaussian output with order up to 95. *Photonix* **2022**, *3*, 4.